



Pergamon

Benzoflavone Activators of the Cystic Fibrosis Transmembrane Conductance Regulator: Towards a Pharmacophore Model for the Nucleotide-Binding Domain

Mark F. Springsteel,^a Luis J. V. Galletta,^b Tonghui Ma,^c Kolbot By,^a Gideon O. Berger,^a Hong Yang,^c Christopher W. Dicus,^a Wonken Choung,^a Chao Quan,^a Anang A. Shelat,^c R. Kiplin Guy,^d A. S. Verkman,^c Mark J. Kurth^{a,*} and Michael H. Nantz^{a,*}

^aDepartment of Chemistry, University of California, Davis, CA 95616, USA

^bLaboratorio di Genetica Molecolare, Istituto Giannina Gaslini, 16148 Genova, Italy

^cDepartments of Medicine and Physiology, Cardiovascular Research Institute, University of California, San Francisco, CA 94143, USA

^dDepartments of Pharmaceutical Chemistry and Cellular and Molecular Pharmacology, University of California, San Francisco, CA 94143, USA

^eChemistry and Chemical Biology Program, University of California, San Francisco, CA 94143, USA

Received 4 February 2003; accepted 22 April 2003

Abstract—Our previous screen of flavones and related heterocycles for the ability to activate the cystic fibrosis transmembrane conductance regulator (CFTR) chloride channel indicated that UCCF-029, a 7,8-benzoflavone, was a potent activator. In the present study, we describe the synthesis and evaluation, using cell-based assays, of a series of benzoflavone analogues to examine structure–activity relationships and to identify compounds having greater potency for activation of both wild type CFTR and a mutant CFTR (G551D-CFTR) that causes cystic fibrosis in some human subjects. Using UCCF-029 as a structural guide, a panel of 77 flavonoid analogues was prepared. Analysis of the panel in FRT cells indicated that benzannulation of the flavone A-ring at the 7,8-position greatly improved compound activity and potency for several flavonoids. Incorporation of a B-ring pyridyl nitrogen either at the 3- or 4-position also elevated CFTR activity, but the influence of this structural modification was not as uniform as the influence of benzannulation. The most potent new analogue, UCCF-339, activated wild-type CFTR with a K_d of 1.7 μ M, which is more active than the previous most potent flavonoid activator of CFTR, apigenin. Several compounds in the benzoflavone panel also activated G551D-CFTR, but none were as active as apigenin. Pharmacophore modeling suggests a common binding mode for the flavones and other known CFTR activators at one of the nucleotide-binding sites, allowing for the rational development of more potent flavone analogues.

© 2003 Elsevier Ltd. All rights reserved.

Introduction

Cystic fibrosis (CF) is the most common lethal genetic disease among Caucasians afflicting one in 2000–2500 Caucasians at birth.¹ CF is caused by mutations in the CF transmembrane conductance regulator (CFTR) protein resulting in chloride-impermeable epithelial cells in the airways, pancreas, intestine and other organs.² Although several novel approaches including gene therapy have attempted to improve CFTR activity in CF

patients,^{3,4} no clinically acceptable therapy has emerged.⁵ Consequently, the identification of small molecule CFTR activators is an important goal of CF research, reasoning that CFTR activators may correct the impaired chloride transport in cells expressing mutant CFTRs in CF patients.^{6,7}

We recently reported the synthesis and cell-based assay of a series of analogues of known CFTR activators.⁸ Chloride conductance was measured using a fluorescence assay in which cells expressing a halide-sensitive green fluorescent protein analogue together with CFTR were treated with test compounds and subjected to halide gradients.⁹ We found that the analogue UCCF-029, a

*Corresponding authors. Tel.: +1-530-752-6357; fax: +1-530-752-8995; e-mail: mhnantz@ucdavis.edu (M. H. Nantz); Tel.: +1-530-752-8192; fax: +1-520-752-8995 e-mail: mjkurth@ucdavis.edu (M. J. Kurth).

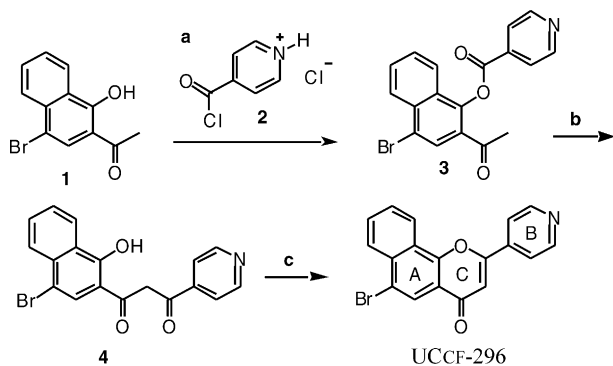
7,8-benzoflavone, was ~ 10 -fold more potent than existing flavones in activating wild type CFTR. Secondary analyses using UCCF-029 indicated that CFTR activation occurred without elevation of cellular cAMP or inhibition of cell phosphatase activity, suggesting a direct interaction with CFTR.

The purpose of the present study was to establish structure–activity relationships for the benzoflavone class of flavonoids, with a goal of identifying compounds having improved potency in the activation of wild type and G551D-CFTR. We selected the G551D-CFTR mutant since, to our knowledge, all reported activators of G551D-CFTR are either flavone- or iso-flavone-derived compounds. We systematically modified the UCCF-029 structure by varying the position of the A-ring benzannulation and the B-ring pyridyl-nitrogen position. We also explored the influence of substituent groups at several A- and B-ring positions. Compounds were screened by our previously reported fluorescence cell-based assay, and the best activators were subjected to dose–response analysis and short-circuit chloride current measurements. The most active analogues were then used to generate a four-point common features pharmacophore model using the HipHop program (Accelrys, Inc). Alignment of this model with other known CFTR agonists suggests a common binding mode at one of the nucleotide binding pockets of CFTR.

Results and Discussion

Compound synthesis

All flavones were synthesized according to the Baker–Venkataraman (B–V) synthesis.^{11,12} A representative synthesis is depicted in Scheme 1. Typically, esterification of *o*-hydroxyacetophenones (e.g., **1**) is followed by treatment with base to promote an intramolecular mixed-Claisen rearrangement which furnishes a diketone (e.g., **4**). In the final step, the flavone C-ring is established via an acid-induced cyclodehydration. All flavones were submitted for testing as 1.0-mM stock solutions in DMSO. Although some required initial warming to dissolve, each compound was soluble at room temperature at this concentration.



Scheme 1. Representative synthesis. Reagents and conditions: (a) **2** (1.2 equiv), pyridine, 0°C to rt, 2 h, 63%; (b) pulverized KOH (1.4 equiv), pyridine, 40°C, 1 h; (c) 4% H₂SO₄ in AcOH, reflux, 1.5 h, 38% (from **3**).

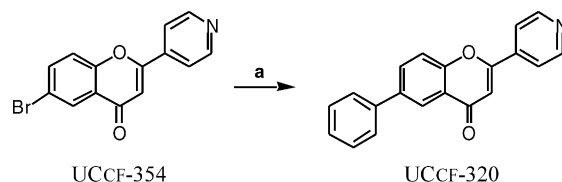
Four of the eight aryl ketone building blocks used in this study were not commercially available and required synthesis. Aryl ketone 1-(5-hydroxy-2,3-dihydrobenzo[1,4]dioxin-6-yl)-ethanone was prepared from gallacetophenone using a straightforward alkylation approach.¹³ A carboxylic acid-to-methyl ketone transformation furnished 2'-hydroxy-3'-acetonaphthone from commercially available 3-hydroxy-2-naphthoic acid.^{14,15} Bromination of 1'-hydroxy-2'-acetonaphthone according to a literature procedure provided the corresponding 4'-bromo-1'-hydroxy-2'-acetonaphthone derivative.^{16,17} Following a literature procedure, reduction of *p*-naphthoquinone, acetylation and Lewis-acid induced Fries rearrangement gave 4'-ethoxy-1'-hydroxy-2'-acetonaphthone.¹⁸ All other aryl ketones used to prepare the panel of analogues were purchased from the Aldrich Chemical Company (Milwaukee, WI, USA).

The 6-bromo-flavone analogues were further diversified using the Suzuki coupling procedure.¹⁹ A representative synthesis is given in Scheme 2.^{20,21} The wide variety of commercially available arylboronic acids makes the Suzuki approach a convenient route for synthesis of novel aryl-substituted flavones.

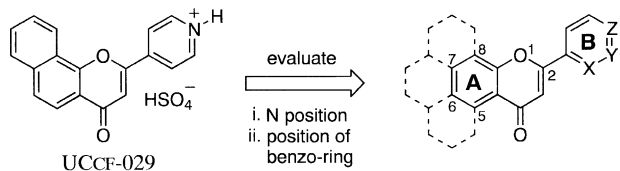
Pharmacology

Tables 1 and 2 and Figures 1–3 summarize the data obtained for the analogues examined in our study. Flavones are referred to by UCCF-OOO (University of California Cystic Fibrosis—compound number) designations when prepared and screened in our labs. Each compound was screened for activation of CFTR in triplicate at 50 μ M together with a low concentration of the cAMP agonist forskolin which itself produced little CFTR activation. Apigenin and 3-isobutyl-1-methyl-xanthine (IBMX) also were included as positive controls. Apigenin²² and IBMX^{7,23} are well-recognized, potent CFTR activators. Phosphate-buffered saline (PBS), apigenin and IBMX CFTR-activating potencies were expressed as slopes of fluorescence versus time curves. The PBS, apigenin and IBMX controls gave maximal slopes of fluorescence change of 11, 40 and 37, respectively.

With UCCF-029 and its conjugate base UCCF-275 as leads, we sought to determine the importance of the two unique structural features: (i) the B-ring 4'-nitrogen and (ii) benzene ring annulation of the A-ring at its 7,8-positions. Furthermore, analogues devoid of one or both of these structural features (e.g., benzoflavones without a B-ring nitrogen) were compared in the matrix. Although UCCF-029 was originally prepared and evaluated as the pyridinium bisulfate salt, we have since



Scheme 2. Representative Suzuki coupling. Reagents and conditions: (a) PhB(OH)₂ (2.1 equiv), 2M Na₂CO₃ (6 equiv), Pd(PPh₃)₄ (2.0 mol%), 1:1 EtOH/PhMe, 90°C, 2 h, 70%.

Table 1. Influence of pyridyl and benzo features^a


Position of benzo ring	X = Y = Z = CH	X = N/Y = Z = CH	Y = N/X = Z = CH	Z = N/X = Y = CH
No ring	Flavone 27	UCCF-324 Toxic	UCCF-343 19	UCCF-284 23
5,6-Benzo	UCCF-315 17	UCCF-344 18	UCCF-345 10	UCCF-289 6.0
6,7-Benzo	UCCF-304 22	UCCF-346 15	UCCF-303 22	UCCF-301 16
7,8-Benzo	UCCF-023 33	UCCF-347 21	UCCF-279 37	UCCF-275 ^b 39

^aEach cell contains the compound identity number and its corresponding CFTR activity data (reported as initial slope and derived as explained in Experimental, Biology).

^bConjugate base of UCCF-029.

determined that the free base (UCCF-275) has identical CFTR activity. Consequently, all pyridyl analogues were evaluated as neutral compounds except where specifically derivatized as alkyl pyridinium salts.

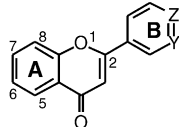
Results of the isomer study are summarized in Table 1. Incorporation of a B-ring nitrogen appears to only minimally activate CFTR by comparison to the corresponding benzo isomer devoid of nitrogen. The influence of the benzannulation modification is more pronounced. Within a given pyridyl series (columns), the most active member of the series is clearly the 7,8-benzo isomer. The greatest distinctions are noted for the 3'- and 4'-pyridyl series where the addition of a 7,8-benzo ring dramatically improves activity. The activities of these two compounds, UCCF-275 and -279, at the 50- μ M assay concentration (Table 1 conditions) are comparable to the potent CFTR activator apigenin, which is roughly 10-fold more potent than genistein.²⁴

Table 2a features additional pyridyl B-ring flavones. The assay data once again reflect the greater influence of the 7,8-benzannulation feature relative to the pyridyl feature in CFTR activation. In this panel, the strongest activators possess a 7,8-benzo ring. Pyridyl analogues without the 7,8-benzo structural feature displayed only minimal CFTR activation (i.e., maximal slope <20). The most active compounds in this panel of analogues contained a 2-furyl substituent at the 6-position. As noted with other substituent series, the activation afforded by the 2-furyl group depends on the presence of the 7,8-benzo ring as well as a pyridyl nitrogen in the B-ring—omission of either of these two features results in lower activities for the 6-(2-furyl) analogues (e.g., compare UCCF-339 vs UCCF-324). Two B-ring 4'-alkylpyridinium salts were prepared and tested to see if a non-titratable positive charge at this position would enhance activity. The data in Table 2a shows that alkylation of the pyridyl ring greatly diminishes CFTR activation (e.g., compare UCCF-029 vs UCCF-340 or UCCF-341). The non-titratable positive charge in these

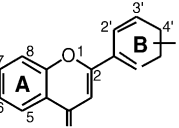
analogues may be expected to influence their transport across biological membranes, and this may account for the lower activity relative to UCCF-029.

Table 2b features flavone and benzoflavone analogues that do not have a pyridyl B-ring. With the exception of the fluoro-isomers, annulation of the A-ring at the 7,8-benzo ring appears to improve activity relative to the benzo-free analogues. None of the non-pyridyl analogues displayed activity comparable to apigenin. Interestingly, the most active analogues in this series were the 3'-F analogue (UCCF-017) and the 4'-F analogues (UCCF-018 and UCCF-349). Since fluorine is a H-bond acceptor,²⁵ these results are consistent with the observations that the presence of a H-bond acceptor—such as a pyridyl nitrogen—in the vicinity of the 4'-position improves activity.²² When the 7,8-benzo ring is replaced with a non-aromatic ethylenedioxo ring fused to the same position, the activity is greatly reduced.

To confirm whether the principal hits in our initial 50 μ M fluorescence assay were sufficiently positive to warrant further investigation, we conducted a dose-response study on the most active compounds using both the aforementioned fluorescence assay and an electrophysiological assay (short-circuit current analysis). We performed dose-response studies on apigenin and analogues UCCF-275, -281, -339, -349 and -353. UCCF-281, -349 and -353 had no significant activity at the 10 μ M dose (data not shown). However, UCCF-275 and UCCF-339 were active at the lower doses. For example, the original plate reader traces for UCCF-339 are depicted in Figure 1a and the corresponding dose-response curve is plotted in Figure 1b. The fitted K_d was 4.8 μ M for UCCF-275, similar to that of apigenin, and 1.7 μ M for UCCF-339 (Fig. 1c). Ussing chamber experiments showed that UCCF-339 evoked large transepithelial Cl^- currents that could be abolished by glibenclamide, a CFTR blocker (Fig. 2a). This benzoflavone was considerably more efficacious than apigenin at similar concentrations (Fig. 2b). Interestingly, in

Table 2. (a) Pyridyl-containing analogues; (b) nitrogen-free analogues


UCCF-	A-Ring substituent	B-Ring modification	Slope ^a
320	6-Phenyl	Y = CH, Z = N	15
321	6-(2-Thienyl)	Y = CH, Z = N	17
322	6-(3-Thienyl)	Y = CH, Z = N	15
324	6-(2-Furyl)	Y = CH, Z = N	19
323	6-(2-Benzofuryl)	Y = CH, Z = N	15
296	7,8-Benzo-6-bromo	Y = CH, Z = N	16
291	7,8-Benzo-6-bromo	Y = N, Z = CH	24
327	7,8-Benzo-6-phenyl	Y = CH, Z = N	12
326	7,8-Benzo-6-phenyl	Y = N, Z = CH	14
330	7,8-Benzo-6-(2-thienyl)	Y = CH, Z = N	22
329	7,8-Benzo-6-(2-thienyl)	Y = N, Z = CH	29
333	7,8-Benzo-6-(3-thienyl)	Y = CH, Z = N	18
332	7,8-Benzo-6-(3-thienyl)	Y = N, Z = CH	23
339	7,8-Benzo-6-(2-furyl)	Y = CH, Z = N	38
338	7,8-Benzo-6-(2-furyl)	Y = N, Z = CH	33
336	7,8-Benzo-6-(2-benzofuryl)	Y = CH, Z = N	16
335	7,8-Benzo-6-(2-benzofuryl)	Y = N, Z = CH	18
350	7,8-Benzo-6-ethoxy	Y = CH, Z = N	16
353	7,8-Benzo-6-hydroxy	Y = CH, Z = N	22
311	7,8-Ethylenedioxo	Y = CH, Z = N	Toxic ^b
029	7,8-Benzo	Y = CH, Z = N·H ₂ SO ₄	38
340	7,8-Benzo	Y = CH, Z = NCH ₃ I	14
341	7,8-Benzo	Y = CH, Z = NCH ₃ CH ₃ I	14



UCCF-	A-Ring substituent	R'	Slope ^a
016	None	2'-F	25
017	None	3'-F	31
018	None	4'-F	33
313	None	4'-Br	14
314	None	4'-OCH ₃	18
290	5,6-Benzo	2'-F	19
316	5,6-Benzo	3'-F	19
044	5,6-Benzo	4'-F	19
268	5,6-Benzo	4'-Br	18
040	5,6-Benzo	4'-OCH ₃	17
317	6,7-Benzo	2'-F	Toxic ^b
318	6,7-Benzo	3'-F	13
300	6,7-Benzo	4'-F	17
319	6,7-Benzo	4'-Br	14
352	6,7-Benzo	4'-OCH ₃	Toxic ^b
025	7,8-Benzo	2'-F	25
282	7,8-Benzo	3'-F	26
281	7,8-Benzo	4'-F	23
271	7,8-Benzo	4'-Br	20
355	7,8-Benzo	4'-OH	15
269	7,8-Benzo	4'-OCH ₃	24
293	7,8-Benzo-6-bromo	2'-F	18
294	7,8-Benzo-6-bromo	4'-F	14
292	7,8-Benzo-6-bromo	4'-OCH ₃	17
297	7,8-Benzo-6-bromo	H	21
325	7,8-Benzo-6-phenyl	2'-F	22
328	7,8-Benzo-6-(2-thienyl)	2'-F	29
331	7,8-Benzo-6-(3-thienyl)	2'-F	17
337	7,8-Benzo-6-(2-furyl)	2'-F	27
334	7,8-Benzo-6-(2-benzofuryl)	2'-F	16
351	7,8-Benzo-6-ethoxy	3'-F	14
348	7,8-Benzo-6-ethoxy	4'-F	16
349	7,8-Benzo-6-hydroxy	4'-F	33
307	7,8-Ethylenedioxo	2'-F	24
308	7,8-Ethylenedioxo	3'-F	23
309	7,8-Ethylenedioxo	4'-F	19
310	7,8-Ethylenedioxo	4'-I	14
305	7,8-Ethylenedioxo	4'-OCH ₃	17
306	7,8-Ethylenedioxo	H	21

^aInitial slope, derived as explained in Experimental, Biology.^bCells detached during the assay.

contrast to apigenin, UCCF-339 did not activate the mutant G551D CFTR (Fig. 2c).

Common features pharmacophore models were derived for all flavones and for the most active (top 10%) flavones. The model generated from all flavones (Fig. 3a) is a subset of the four-point model describing the most active flavones (Fig. 3b). The four-point model has the following features: a hydrogen bond acceptor (A), an aromatic ring (B), and two hydrophobic groups (C and D). The inter-atomic distances between the center-of-mass coordinates of each pharmacophore point are as follows: A–B (3.0 Å), B–C (5.4 Å), B–D (3.2 Å). The angles between the pharmacophore points are: A–B–C (88.9°), A–B–D (159.3°), C–B–D (111.8°). The improper torsion angle, A–B–D–C, is 180.0°, indicating a planar geometry. The additional hydrophobic pharmacophore feature present in the model derived from the most active flavones (point D) reflects the increase in activity due to benzannulation at the 7,8-position.

We then applied our model to analysis of other known CFTR agonists. Recently, Ma et al.¹⁰ reported a novel set of CFTR agonists with diverse scaffolds. Three of the 17 most active compounds were excluded from our study because they appeared to activate CFTR indirectly by elevating cellular cAMP. The remaining 14 strongly active compounds from the Ma report were overlaid on the four point pharmacophore model and 11 of the 14 compounds aligned well to all four points of the flavone pharmacophore (see Fig. 3c for examples of the alignments). Three compounds, CFTRact-05, CFTRact-09, and CFTRact-13, failed to map the correct chemical functionalities to each of the four pharmacophore points. Furthermore, the flavone pharmacophore overlaps nicely with known CFTR agonists such as adenosine and the xanthine CPX. Figure 3d shows the alignment of these two compounds: the xanthine maps well to all points, whereas the heterocyclic ring and sugar of adenosine occupy three of the four pharmacophore points. These compounds have been shown to bind the nucleotide-binding pocket of CFTR,²⁶ suggesting that the flavones and some of the previously identified CFTR agonists share a common binding mode at this site. Indeed, flavonoids have been shown to bind the ATP-binding domains of other biologically important molecules, including the cyclin-dependent kinase 2,²⁷ mouse P-glycoprotein²⁸ and a haematopoietic cell kinase.²⁹ Further understanding of the interactions at the nucleotide-binding domain of CFTR could enable design of small molecule effectors targeting pathophysiological CFTR mutations.

Conclusion

We prepared and screened a panel of benzoflavones for activation of wild type CFTR. The structures were selected to probe the relevance of A-ring benzannulation and a B-ring pyridyl-nitrogen, both structural features that were identified by our previous screening of MPB-07–genistein hybrid analogues. The data shows that benzannulation at the 7,8-positions of the flavone

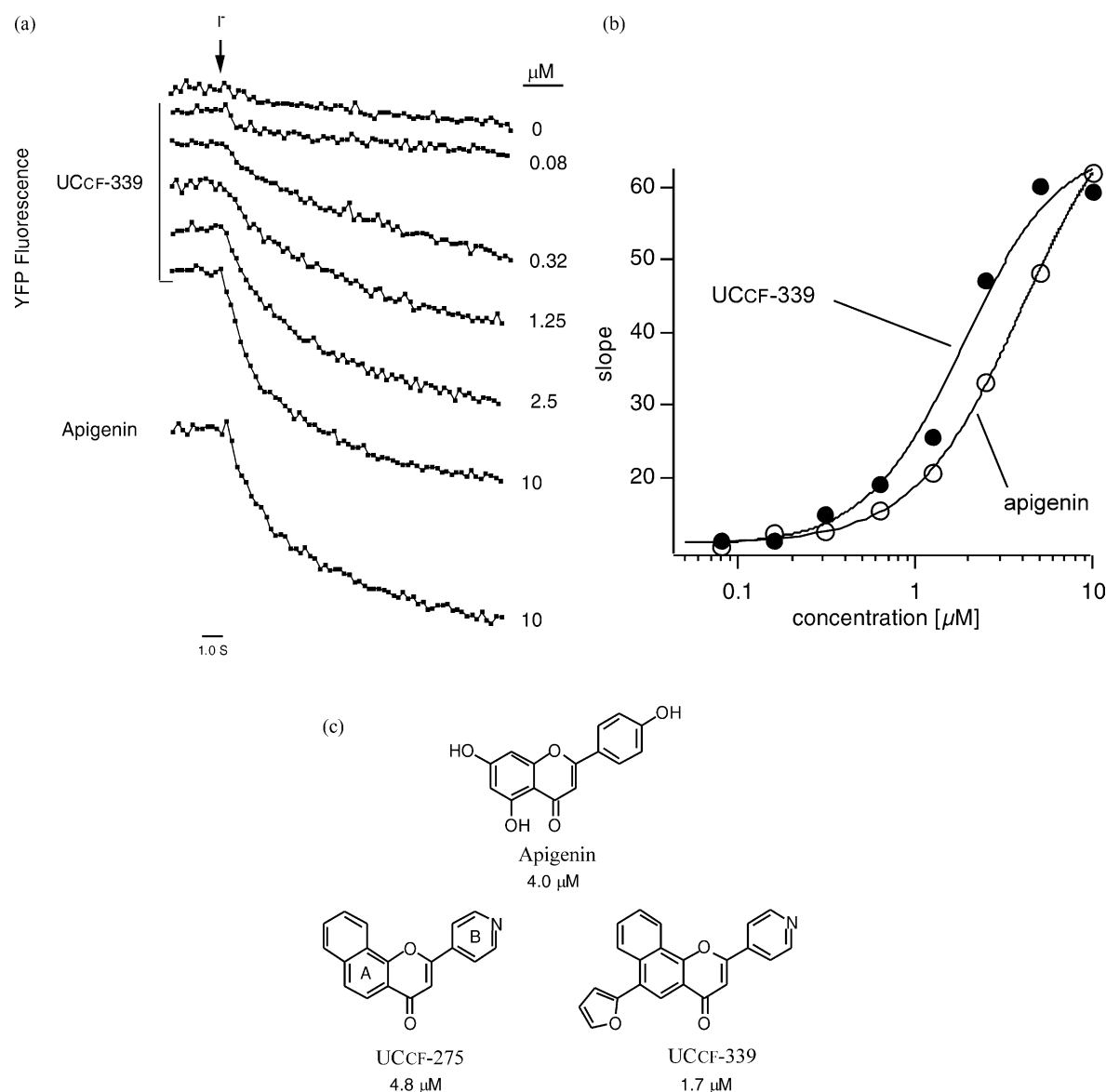


Figure 1. CFTR activation by UCCF-339 and apigenin: (a) representative fluorescence traces showing CFTR-dependent I^- influx by UCCF-339 at different concentrations and by apigenin (at 10 μM); (b) corresponding dose–response relationships for UCCF-339 and apigenin, data fitted with the Hill equation; (c) most active compounds with respective K_d in μM .

scaffold significantly improves the activation of wild-type CFTR. The presence of a rigid π -system in this domain is uniformly superior to benzannulation at other A-ring positions. The pyridyl B-ring appears less influential in activating CFTR than the 7,8-benzannulation. Furthermore, modifications of the flavone B-ring with a pyridyl-nitrogen or fluorine substituent at positions 3' or 4' are equally well tolerated. Two benzo-flavone analogues displayed activity comparable to apigenin and better than IBMX at the 50- μM concentration. Dose–response data in both fluorescence and electrophysiological studies confirm that UCCF-339 has 4-fold higher maximal activity than UCCF-029 and apigenin, the most potent flavonoid activators of wild-type CFTR. Computational analysis of the SAR data led to a consensus common features pharmacophore model that provides an emerging picture of the binding site for activators of CFTR.

Experimental

General synthesis methods. ^1H and spectra were recorded in CDCl_3 on a Mercury (300 MHz) and an Inova (400 MHz) spectrometer with TMS as an internal standard. Infrared spectra of neat samples were recorded on a Mattson Genesis II FTIR. Melting points were determined using an Electrothermal digital melting point apparatus and are uncorrected. Elemental analyses were performed by Midwest Microlabs, Indianapolis, IN, USA. Flash column chromatography was carried out using EM Science silica gel 60 (230–400 mesh). TLC was performed on Merk silica gel 60 F₂₅₄ plates and visualized under a UV lamp. THF was distilled from sodium benzophenone ketyl immediately prior to use, CH_2Cl_2 was distilled from calcium hydride immediately prior to use and all other reagents were used as purchased from Aldrich, Acros and Fisher.

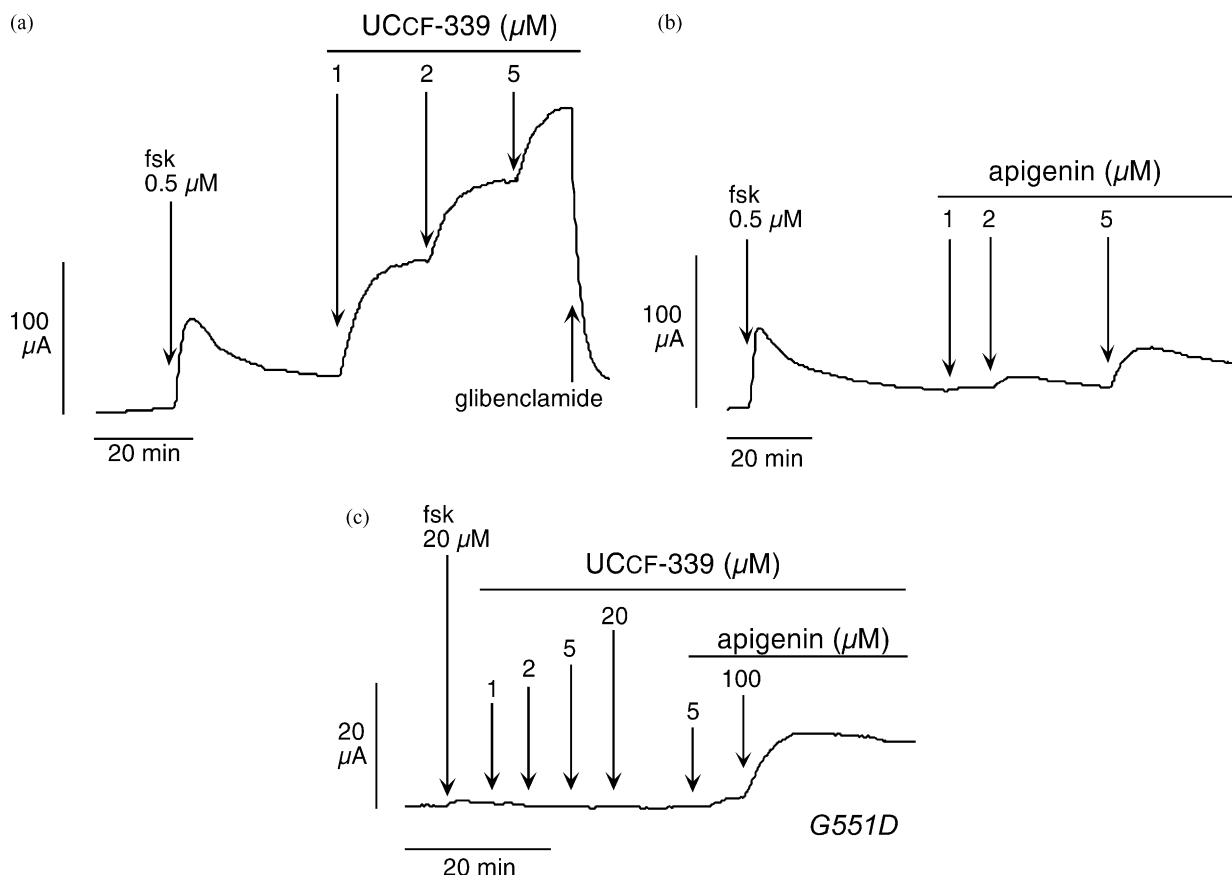


Figure 2. Measurement of CFTR-dependent Cl^- transport by short-circuit current experiments. (a,b) Effect of increasing concentrations of UCCF-339 or apigenin on FRT cells expressing wild-type CFTR. Forskolin was applied at a low concentration to provide a minimal CFTR phosphorylation. (c) Stimulation of FRT cells expressing G551D-CFTR by high forskolin concentration followed by UCCF-339 and apigenin.

Representative B-V synthesis. Step 1: 2-acetyl-4-bromonaphthyl-pyridine-4-carboxylate (3). To a solution of 2-acetyl-4-bromo-1-naphthol (2.02 g, 7.62 mmol) in pyridine (40 mL) at 0°C was added isonicotinoyl chloride HCl (1.72 g, 9.18 mmol) in one portion. After 5 min, the reaction was warmed to room temperature and stirred an additional 2 h. The reaction was quenched by addition of a 1:1 mixture of 5% aq HCl/crushed ice (40 mL). The resultant precipitate was collected by filtration and washed with ice cold water. The precipitate was then dissolved in EtOAc (100 mL) and the solution was washed with brine (20 mL) and dried (Na_2SO_4). The solvents were removed and the residue was purified by chromatography with gradient elution (10–75% EtOAc in CH_2Cl_2) to obtain ester **3** (1.77 g, 63%) as a white solid; mp $150\text{--}151^\circ\text{C}$; TLC, R_f (EtOAc) 0.46; IR 3041, 1737, 1687 cm^{-1} ; ^1H NMR (300 MHz) δ 8.93 (dd, $J=4.1, 1.8$ Hz, 2H), 8.28 (d, $J=8.8$ Hz, 1H), 8.21 (s, 1H), 8.11 (dd, $J=4.7, 1.8$ Hz, 2H), 8.01 (d, $J=8.2$ Hz, 1H), 7.75 (ddd, $J=7.6, 7.0, 1.2$ Hz, 1H), 7.62 (ddd, $J=8.2, 7.0, 1.2$ Hz, 1H), 2.62 (s, 3H); ^{13}C NMR (75 MHz) δ 195.7, 163.6, 151.0, 145.5, 136.1, 134.6, 130.2, 128.9, 128.4, 128.3, 127.7, 126.4, 123.4, 123.2, 120.7, 29.8. Anal. calcd $\text{C}_{18}\text{H}_{12}\text{BrNO}_3$: C, 58.40; H, 3.27; N, 3.78. Found: C, 58.29; H, 3.54; N, 3.56.

Steps 2 + 3: 6-bromo-2-(4-pyridyl)benzo[*h*]4H-chromen-4-one (UCCF-296). To a solution of 2-acetyl-4-bromonaphthylpyridine-4-carboxylate (1.63 g, 4.39 mmol) in pyridine (11 mL) at 40°C was added freshly pulverized KOH (340 mg, 6.1 mmol) in one portion. After 1 h, the reaction was quenched by addition of 5% aq HCl (7 mL). The resultant precipitate was collected by filtration and washed with ice cold water. The precipitate was dried and then dissolved in glacial acetic acid (22 mL). Conc. sulfuric acid (0.9 mL) was added and the reaction mixture was heated to reflux. After 1.5 h, the mixture was cooled to room temperature and quenched by pouring over 50 g crushed ice. The precipitate was filtered and washed with ice cold water. The precipitate was dissolved in a mixture of CH_2Cl_2 (100 mL) and MeOH (50 mL) and then the solution was washed with sat. NaHCO_3 (3×25 mL). The organic fraction was dried (Na_2SO_4), concentrated by rotary evaporation, and the residue was purified by chromatography, eluting with 5% MeOH in CH_2Cl_2 , to yield UCCF-296 (0.58 g, 38%) as an off-white solid; mp $279\text{--}280^\circ\text{C}$; TLC, R_f 0.51 (5% MeOH in CH_2Cl_2). IR 3060, 3020, 1654 cm^{-1} ; ^1H NMR (300 MHz) δ 8.90 (d, $J=5.5$ Hz, 2H), 8.60 (ddd, $J=8.1, 1.6, 0.8$ Hz, 1H), 8.45 (s, 1H), 8.36 (ddd, $J=8.0, 1.6, 0.6$ Hz, 1H), 7.89–7.78 (m, 4H), 7.05 (d, $J=0.6$ Hz, 1H);

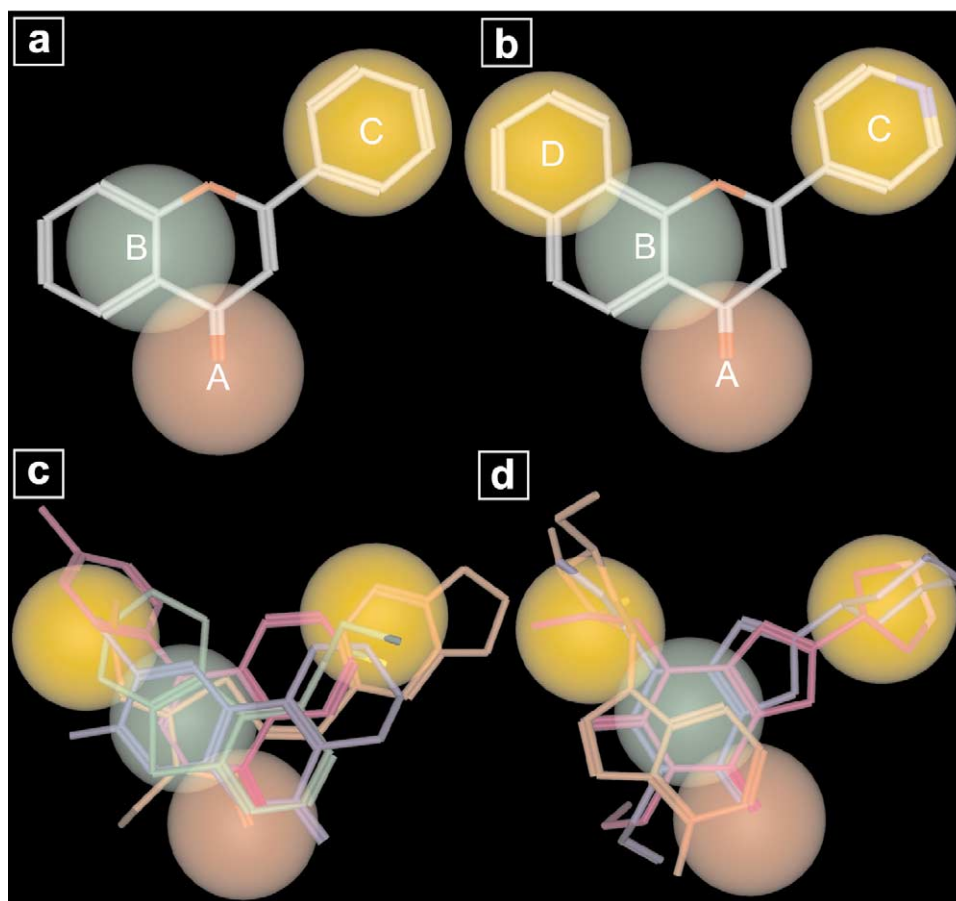


Figure 3. Common features pharmacophore modeling from the flavone series of CFTR activators and comparison to other channel activators. (a) The consensus pharmacophore model derived from all flavones in the study, shown aligned to the parent flavone. Pharmacophore features are shown as labeled, colored spheres: red (A, hydrogen bond acceptor), green (B, aromatic ring), orange (C, hydrophobic group). (b) The four-point pharmacophore derived from the most active flavones (top 10%) in this study, shown aligned to UCCF-029. The hydrophobic feature corresponding to point D reflects the importance of benzannulation at the 7,8-position for activity. (c) Alignment of CFTRact04 (red), CFTRact14 (green), CFTRact12 (blue), and CFTRact17 (purple) to the four-point pharmacophore model from (b). (d) Alignment of adenosine (red) and the xanthines CPX (purple) and DAX (blue) to the four-point model from (b).

^{13}C NMR (100 MHz) δ 176.7, 160.3, 153.0, 151.2, 139.2, 134.5, 131.0, 128.4, 128.3, 125.3, 124.4, 122.7, 121.1, 120.6, 119.9, 110.8. Anal. calcd $\text{C}_{18}\text{H}_{10}\text{BrNO}_2$: C, 61.39; H, 2.86; N, 3.98. Found: C, 61.11; H, 2.85; N, 3.93.

Representative Suzuki coupling: 6-phenyl-2-(4-pyridyl)4H-chromen-4-one (UCCF-320). To a degassed (Ar) mixture of 6-bromo-2-(4-pyridyl)4H-chromen-4-one (151 mg, 0.500 mmol), phenylboronic acid (125 mg, 1.03 mmol) and 2 M Na_2CO_3 (1.5 mL) in EtOH (2.5 mL) and toluene (2.5 mL) at room temperature was added $\text{Pd}(\text{Ph}_3\text{P})_4$ (11.5 mg, 9.95 μM). After heating to reflux 2 h, the reaction was cooled to room temperature and diluted with EtOAc (50 mL) and water (10 mL). The layers were separated and the organic fraction was washed with brine (1 \times 25 mL) and dried (Na_2SO_4). After removal of the solvents, the crude material was purified via recrystallization from EtOAc to yield UCCF-320 (122 mg, 70%) as white crystals; mp 204–205 $^\circ\text{C}$, TLC, R_f (EtOAc) 0.26. IR 3047, 1636, 1611 cm^{-1} . ^1H NMR (300 MHz) δ 8.81 (d, $J=5.3$ Hz 2H), 8.41 (d, $J=2.3$ Hz, 1H), 7.96 (dd,

$J=8.8, 2.3$ Hz, 1H), 7.76 (d, $J=5.3$ Hz, 2H), 7.65 (dd, $J=4.1, 3.5$ Hz, 2H), 7.62 (s, 1H), 7.49–7.36 (m, 3H), 6.91 (s, 1H); ^{13}C NMR (75 MHz) δ 117.9, 160.4, 155.4, 150.8, 139.0, 138.9, 138.7, 133.0, 129.0, 128.0, 127.1, 124.1, 123.5, 119.7, 118.7, 109.2. Anal. calcd $\text{C}_{20}\text{H}_{13}\text{NO}_2$: C, 80.25; H, 4.38; N, 4.68. Found: C, 80.18; H, 4.37; N, 4.72.

Computational chemistry

Common features pharmacophore models for all flavones and the top 10% most active flavones were generated using the HipHop module in Catalyst (Accelrys, Inc.). Briefly, the HipHop algorithm accepts a collection of conformational models for each molecule and attempts to align the molecules based on a set of chemical features, such as hydrogen bond donor/acceptor, aromatic ring, or hydrophobe. Pharmacophore features are assigned where like chemical features map to the same region in space, within a user-defined tolerance. Prior to input into HipHop, each molecule was subjected to geometry optimization using quantum

mechanics at the HF/6-31G* level of theory (Gaussian 98). Conformational models were generated using the Confirm algorithm with the Best option and default parameters (Accelrys, Inc.). Molecules were aligned to the pharmacophore models and viewed using the Compare/Fit module in Catalyst (Accelrys, Inc.). Alignments were viewed and analyzed using the program MOE (Chemical Computing Group, Inc.).

Biology

Halide transport assay. Fisher rat thyroid (FRT) cells stably co-expressing human wild-type CFTR and the yellow fluorescent protein YFP-H148Q were cultured and assayed as described previously.¹⁰ Briefly, cells were plated in 96-well microplates and, after 24–48 h, washed with PBS and incubated for 15 min with 40 μ L of the same solution containing 100 nM forskolin with or without compounds to be tested or reference CFTR activators (apigenin and IBMX) at various concentrations. The microplates were then processed in a FluoStar fluorescence microplate reader (BMG Lab Technologies) equipped excitation/emission filters for yellow fluorescent protein (Chroma) and two syringe pumps for liquid addition. Each well fluorescence was read for 14 s with a sampling time of 0.2 s. After 2 s of fluorescence reading, 165 μ L of a PBS containing 137 mM NaI instead of NaCl was added to measure CFTR-dependent fluorescent quenching. The decay of fluorescence in each well was fitted with a third-order polynomial to derive the initial fluorescence slope at the time of iodide addition.

Short-circuit current measurements. FRT cells expressing wild-type or G551D-CFTR were plated at high density on Snapwell (Corning-Costar) permeable inserts as described previously.¹⁰ After 7–10 days, Snapwell inserts were mounted in a modified Ussing chamber. The basolateral side was filled with a Ringer solution containing: 130 mM NaCl, 2.7 mM KCl, 1.5 mM KH_2PO_4 , 1 mM CaCl_2 , 0.5 mM MgCl_2 , 10 mM Na-Hepes (pH 7.3), and 10 mM glucose. The apical side contained a similar solution in which half of NaCl was replaced with sodium gluconate and the CaCl_2 increased to 2 mM. The basolateral membrane of FRT cells was permeabilized with 250 $\mu\text{g/mL}$ of amphotericin B for 30 min. Both sides were connected to a voltage clamp (World Precision Instruments) by means of voltage-sensing and current-passing Ag/AgCl electrodes. Short-circuit current data were converted in digital form and stored on an Apple personal computer.

Acknowledgements

This work was supported by a drug discovery grant from the Cystic Fibrosis Foundation. We thank Mr. Sung Hee Hwang for assistance with compound preparations. A.A.S. is supported by the National Defense Science and Engineering Graduate Fellowship.

References and Notes

- Young, L. Y.; Koda-Kimble, M. A. *Applied Therapeutics, The Clinical Use of Drugs*, 6th Ed.; Applied Therapeutics: Vancouver, NA, 1995; p 100.1.
- Pilewski, J. M.; Frizzell, R. A. *Physiol. Rev.* **1999**, *79*, S215.
- Liu, X.; Jiang, Q.; Mansfield, S. G.; Puttaraju, M.; Zhang, Y.; Zhou, W.; Cohn, J. A.; Garcia-Blanco, M. A.; Mitchell, L. G.; Engelhardt, J. F. *Nat. Biotechnol.* **2002**, *20*, 47.
- Kitson, C.; Alton, E. *Expert Opin. Invest. Drugs* **2000**, *9*, 1523.
- Marshall, E. *Science* **2000**, *287*, 565.
- Zeitlin, P. L. *J. Clin. Invest.* **1999**, *103*, 447.
- Schultz, B. D.; Singh, A. K.; Devor, D. C.; Bridges, R. J. *Physiol. Rev.* **1999**, *79*, S109.
- Galiotta, L. J. V.; Springsteel, M. F.; Eda, M.; Niedzinski, E. J.; By, K.; Haddadin, M. J.; Kurth, M. J.; Nantz, M. H.; Verkman, A. S. *J. Biol. Chem.* **2001**, *276*, 19723.
- Galiotta, L. J. V.; Jayaraman, S.; Verkman, A. S. *Am. J. Physiol. Cell Physiol.* **2002**, *281*, C1734.
- Ma, T.; Vetrivel, L.; Yang, H.; Pedemonte, N.; Zegar-Moran, O.; Galiotta, L. J. V.; Verkman, A. S. *J. Biol. Chem.* **2002**, *277*, 37235.
- Baker, W. J. *Chem. Soc.* **1933**, 1381.
- Mahal, H. S.; Venkataraman, K. *J. Chem. Soc.* **1934**, 1767.
- Dallacker, F.; Wersch, J. V. *Chem. Ber.* **1972**, *105*, 3301.
- Brunner, H.; Schiebling, H. *Bull. Soc. Chim. Belg.* **1994**, *103*, 119.
- Banu, H. S.; Pitchumani, K.; Srinivasan, C. *Tetrahedron* **1999**, *55*, 9601.
- Furniss, B. S.; Hannaford, A. J.; Smith, P. W. G.; Tatchell, A. R. *Vogel's Textbook of Practical Organic Chemistry*, 5th Ed.; John Wiley & Sons: New York, 1989; p 980.
- Paranjape, M. V.; Wadodkar, K. N. *Indian J. Chem.* **1981**, *20B*, 808.
- Boyer, J. L.; Krum, J. E.; Myers, M. C.; Fazal, A. N.; Wigal, C. T. *J. Org. Chem.* **2000**, *65*, 4712.
- Suzuki, A. *Pure Appl. Chem.* **1985**, *57*, 1749.
- Wei, Z.-Y.; Brown, W.; Takasaki, B.; Plobeck, N.; Delorme, D.; Zhou, F.; Yang, H.; Jones, P.; Gawell, L.; Gagnon, H.; Schmidt, R.; Yue, S.-Y.; Walpole, C.; Payza, K.; St-Onge, S.; Labarre, M.; Godbout, C.; Jakob, A.; Butterworth, J.; Kamassah, A.; Morin, P.-E.; Projean, D.; Ducharme, J.; Roberts, E. *J. Med. Chem.* **2000**, *43*, 3895.
- Muller, D.; Fleury, J.-P. *Tetrahedron Lett.* **1991**, *32*, 2229.
- Illek, B.; Lizarzaburu, M. E.; Lee, V.; Nantz, M. H.; Kurth, M. J.; Fischer, H. *Am. J. Physiol. Cell Physiol.* **2000**, *279*, C1838.
- Bulteau, L.; Derand, R.; Mettey, Y.; Metaye, T.; Morris, M. R.; McNeilly, C. M.; Folli, C.; Galiotta, L. J. V.; Zegar-Moran, O.; Pereira, M. M. C.; Jouglu, C.; Dormer, R. L.; Vierfond, J. M.; Joffre, M.; Becq, F. *Am. J. Physiol. Cell Physiol.* **2000**, *279*, C1925.
- Illek, B.; Zhang, L.; Lewis, N. C.; Moss, R. B.; Dong, J. Y.; Fischer, H. *Am. J. Physiol. Cell Physiol.* **1999**, *277*, C833.
- Diamond, J. M.; Wright, E. M. *Proc. Royal Soc., Ser. B* **1969**, *172*, 273.
- Cohen, B. E.; Lee, G.; Jacobson, K. A.; Kim, Y.-C.; Huang, Z.; Sorscher, E. J.; Pollard, H. B. *Biochemistry* **1997**, *36*, 6455.
- Azevedo, W. F. D., Jr.; Mueller-Dieckmann, H.-J.; Schulze-Gahmen, U.; Worland, P. J.; Sausville, E.; Kim, S.-H. *Proc. Natl. Acad. Sci. U.S.A.* **1996**, *93*, 2735.
- Conseil, G.; Baubichon-Cortay, H.; Dayan, G.; Jault, J.-M.; Barron, D.; Di Pietro, A. *Proc. Natl. Acad. Sci. U.S.A.* **1998**, *95*, 9831.
- Sicheri, F.; Moarefi, I.; Kuriyan, J. *Nature* **1997**, *385*, 602.